A Fast Approach to Best Scanline Search of Airborne Linear Pushbroom Images

Mi Wang, Fen Hu, Jonathan Li, and Jun Pan

Abstract

The linear pushbroom camera has become one of the most important imaging sensors in today's photogrammetry and remote sensing practices. Airborne digital sensors (ADS) or three-line scanner (TLS) imaging system such as the ADS40 from Leica Geosystems and STARIMAGER from STARLABO Corporation use the pushbroom technique to collect high-resolution, multi-channel seamless image strips. As we know, the object-to-image coordinate computation serves as a core step during the process of photogrammetric images. However, each scanline captured by a linear pushbroom sensor has six exterior orientation (EO) parameters at the corresponding instant of exposure. The image point coordinates will not be accurately calculated through colinearity equations unless reasonable EO parameters are determined. Therefore, the best scanline search (BSS) has direct effects on efficiency of object-to-image coordinate computation during image processing. This paper addresses a fast BSS method based on the novel central perspective plane of scanline (CPPS) constraints. The search process is simply performed through analytical geometric calculations, which can significantly improve the efficiency of the object-to-image coordinate computation. The feasibility and robustness of the proposed method have been verified using ADS40 and STARIMAGER images. Experimental results show that the proposed method improves scanline search speed considerably with the time cost decreased by nearly 85 percent compared with the traditional methods.

Introduction

Line pushbroom sensor systems have been already widely used on satellite platforms, and they have entered the scene as airborne imaging systems in the last few years. In comparison to matrix array CCD sensor systems, the linear array CCD principle offers some distinct advantages which have caused a number of camera manufacturers to use this principle for their new digital aerial cameras. One of the key advantages lies in the fact that a very large image format, as it is required in the traditional aerial photogrammetric practice, can more easily be generated (Sandau *et al.*, 2000; Hinz *et al.*, 2000; Heier *et al.*, 2002; Leberl *et al.*, 2002; Leberl *et al.*, 2003; Fricker, 2001; Koichi *et al.*, 2004). The first commercial line scanner Airborne Digital Sensor (ADS40) was developed by LH Systems (now Leica Geosystems) jointly with German Aerospace Centre (DLR) (Reulke *et al.*, 2000, Sandau *et al.*, 2000). In the year 2000, STARLABO Corporation, Tokyo designed the airborne Three-Line-Scanner (TLS) system, jointly with the Institute of Industrial Science, University of Tokyo (Murai and Matsumoto, 2000). The system was later called STARIMAGER. These two commercial digital cameras both adopt the linear pushbroom technique and have the capacity to simultaneously capture high-quality panchromatic, near infrared, and multispectral seamless image sequences from forward, nadir, and back viewing-angles. The noticeable potential of airborne linear pushbroom sensors in both data acquisition and application aspects compared with the traditional frame-based cameras have attracted great attention and many concerns from researchers of many countries (Haala *et al.*, 2000; Gruen and Zhang, 2001; Gruen and Zhang, 2002; Gruen and Zhang, 2003; Koichi *et al.*, 2004; Reulke *et al.*, 2006; Cramera, 2006; Li *et al.*, 2007). Several ADS40 systems have been purchased and used in China for domestic digital aerial surveying business and academic research projects. Experiments and practices indicate that the linear pushbroom images do have tremendous potential for measuring and interpreting the comprehensive conditions of the ground surface. However, the introduction of digital line sensors into the field of aerial photogrammetry has provided a challenging research area for photogrammetrists due to its fairly new sensor geometry and wide-range of spectral data availability.

In aerial photogrammetry, the coordinate computation of an image point corresponding to the ground point plays as a fundamental link in many photogrammetric applications, such as the generation of epipolar images and orthoimagery, as well as the epipolar images-based stereoscopic measurement and mapping. Nevertheless, compared with the traditional frame-based photos or CCD matrix images, the airborne linear pushbroom images have a much more complex situation to be faced with (Morgan *et al.*, 2004; Chen *et al.*, 2007). It is well known that airborne linear pushbroom sensor is capable of providing continuous long "pixel carpet" with a GSD (Ground Sampling Distance) resolution up to decimeter level (Sandau *et al.*, 2000).

Mi Wang, Fen HU, and Jun Pan are with the State Key Laboratory of Information Engineering in Surveying, Mapping and Remote Sensing, Wuhan University, 129 Luo Yu Road, Wuhan, Hubei, China 430079 (hufen1984@163.com).

Jonathan Li is with the Department of Geography and Environmental Management, Faculty of Environment, University of Waterloo, 200 University Avenue West, Waterloo, Ontario, Canada N2L 3GI.

Photogrammetric Engineering & Remote Sensing
Vol. 75, No. 9, September 2009, pp. 1059–1067.

0099-1112/09/7509–1059/$3.00/0

Furthermore, image strips simultaneously captured by line sensors with forward, nadir, and back viewing-angles along the flight have high-overlapping ground coverage, thus inducing the mass data characteristic of airborne linear pushbroom images, which leads to a extremely high burden on image data processing. Typically, one scene of linear pushbroom imagery contains at least tens of thousands of scanlines; and moreover, due to the linear pushbroom imaging mode, each scanline captured by line sensor possesses six exterior orientation (EO) parameters at its corresponding exposure moment. The coordinates of the image point will not be accurately calculated through the rigorous mathematical sensor model (i.e., colinearity equations) unless reasonable EO parameters are determined. Therefore, the best scanline search (BSS) becomes an issue which has a significant effect on efficiency of object-to-image coordinate computation.

The image-space-based sequential search can be considered as the most original method developed and has been used to solve the BSS issue of satellite linear pushbroom images. As shown in Figure 1, according to the criterion that the image point coordinates calculated with mathematical sensor model should be theoretically equal with the calibrated coordinates of the corresponding imaging CCD detector, the search process is carried out sequentially in image space with a constant scanline interval, based on iterative object-to-image coordinates calculations and verifications. However, since one scene of image contains large number of scanlines, such a method could be imaginably time-consuming and inefficient, thus unsuitable for practical use. In recent years, new methods have been proposed to try and reduce the search region of image space and improve the searching efficiency, such as the bisecting window search (Liu and Wang, 2007), the local affine-transformation window search provided by Leica Geosystems software developing kit, as well as the optimized image-space sequential search (Zhao and Li, 2006).

The bisecting window search method has recently been proposed and successfully employed in the indirect orthorectification of ADS40 Level-0 imagery, and has received much more attention for improving the search efficiency from both speed and accuracy aspects. The first step of this method is to choose an image interval between the first and the last scanline as the initial search window. Then, it iteratively halves the search window by comparing the three pairs of image point coordinates calculated through colinearity equations, respectively, by employing the EO parameters of the first, the middle, and the last scanline of the search window. Finally, a sequential search is carried out in the final bisecting window within a threshold size. The affine transformation-based window search is another method once emerged in the pseudo-code provided by the Leica Geosystems software development kit. This method is based on the approximate local affine-transformation between object space and image space of linear pushbroom images (Zhang, 2005; Poli, 2005). Photogrammetric rays of linear pushbroom image in the direction of flight can be regarded as parallel projection to a certain extent, so the affine transformation relationship between ground space and image space can be established approximately. Relying on the considerable initial search value provided by iterative object-to-image affine transformation, the sequential search range of image-space can be effectively decreased.

By evaluating the performance of the above optimization methods most currently employed, it is found that although they all make achievements in providing proper initial scanline for the post sequential search process thus optimizing the original image-space sequential search method in different degrees, the calculation amount spent in obtaining proper initial scanline is also somewhat high to some extent, especially for the affine transformation based window search, as several iterations of colinearity equation-based computations are still needed to determined the local affine transformation parameters. Besides, no matter what search speedup approaches are considered with these methods, for every best scanline search, there is still the need for multiple colinearity equation-based computations. The main problem is that they all merely consider the image-space-based solution strategy which is rooted on the iterative computations through colinearity equations. Therefore, the fundamental solution is to explore some more effective search criterions to replace the existing image-space-oriented one based on which the BSS process is accomplished.

This paper proposes a fast method for BSS issue of airborne linear pushbroom images, based on the novel central perspective plane of scanline (CPPS) constraints of object space. The reminder of the paper is organized as follows. The following section introduces the theoretical background followed by a description of the principle of the proposed method are described. The next sections describe the detailed processing procedures of our strategy followed by experimental results with discussion and conclusions.

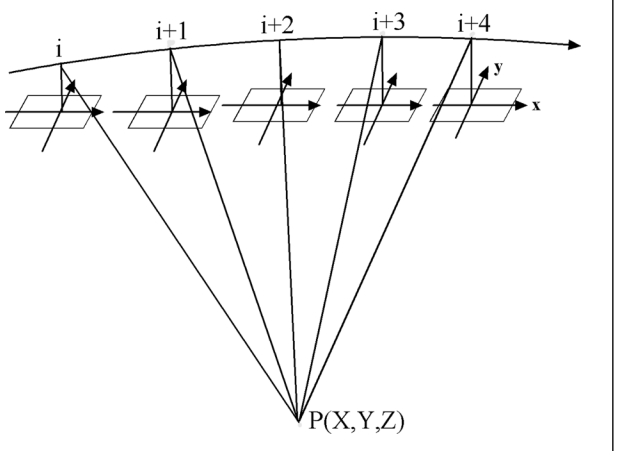

Figure 1. Image-space sequential search.

Theoretical Background

Geometric Sensor Model

For airborne linear pushbroom sensors such as the ADS40 and STARIMAGER, the backward, nadir, and forward viewing-angle pushbroom imaging mode (see Figure 2) is implemented through the combination of optical system and CCD line sensors mounted on the focal planes. While the camera platform moves along the flight direction, each line sensor captures scanlines perpendicular to the flight trajectory, and successive scanlines are acquired and stored one after one to form the whole image strip (Wolf and Dewitt, 2000; Poli, 2005).

Based on the pushbroom imaging mode of each sensor line, on one hand, the geometric sensor model in the direction of flight can be approximately considered to be a parallel perspective, which is somewhat derived from the relatively small field-angle of the line sensor (Zhang, 2005). On the other hand, the central perspective geometry is still rigorous to define the sensor model in the direction of line sensor, i.e., colinearity equations, the mathematical

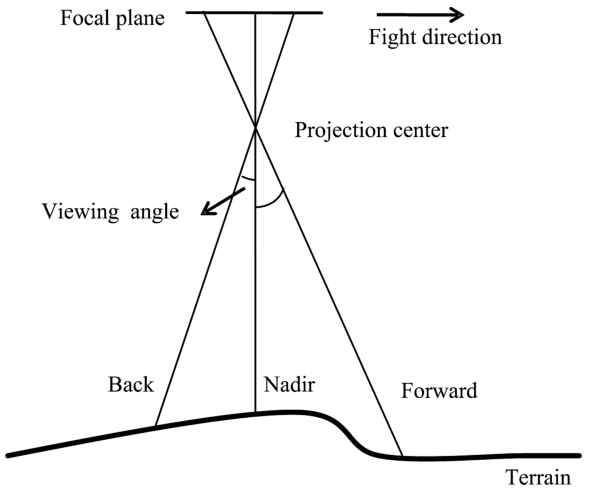

Figure 2. Pushbroom imaging mode of the three-line-scanner.

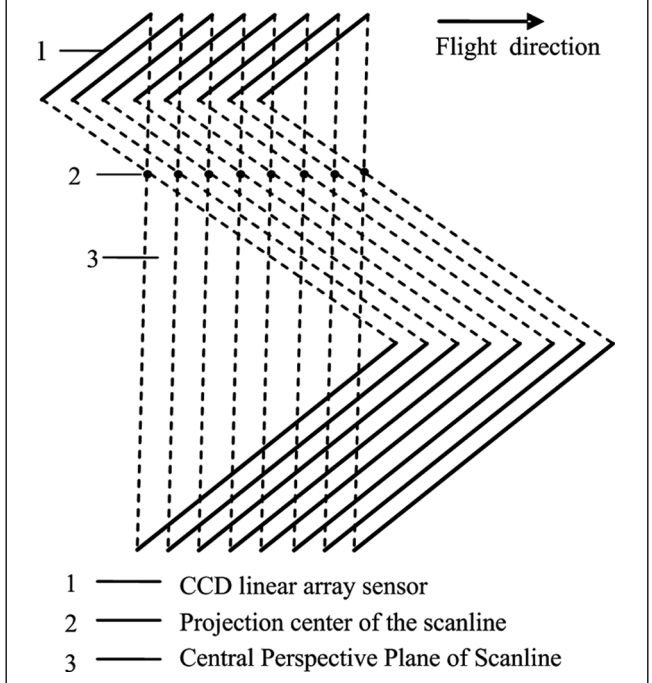

Figure 3. Central perspective plane of scanline (CPPS).

model used to describe the relationship between object space and image space as defined as follows (Wolf and Dewitt, 2000):

$$x = -f\frac{a_1(X - Xs_i) + b_1(Y - Ys_i) + c_1(Z - Zs_i)}{a_3(X - Xs_i) + b_3(Y - Ys_i) + c_3(Z - Zs_i)}$$
$$y = -f\frac{a_2(X - Xs_i) + b_2(Y - Ys_i) + c_2(Z - Zs_i)}{a_3(X - Xs_i) + b_3(Y - Ys_i) + c_3(Z - Zs_i)} \quad (1)$$

where X, Y, Z are the ground coordinates of a point, x, y are the image coordinates of the point, f is the focal length, Xs_i, Ys_i, Zs_i are the coordinates of the exposure station of scanline indexed with i, and a_i, b_i, c_i ($i = 1, 2, 3$) are the elements of rotate matrix derived from EO angular parameters of scanline indexed with i.

CPPS Constraints

As illustrated in Figure 3, the supposed central perspective plane of scanline (CPPS) is the spatial plane determined by the CCD line sensor and the projection center of each scanline at the corresponding instant of exposure. Under normal conditions, in order to acquire the qualified and applicable pushbroom images, some rules should be adhered to during the imaging process: (a) the CPPSs are approximately parallel and will not intersect with each other in the effective imaging range of object space, (b) the speed of the aircraft must be as stable as possible, and (c) the distance between the adjacent planes should be approximately equal.

Accordingly, a novel, fast BSS method based on the CPPS constraints of object space can be derived: as shown in Figure 4, if P_l and P_r, the two nearest neighboring CPPSs of the ground point (X, Y, Z) are searched out, the best scanline can be positioned by object-space interpolation based on P_l and P_r. In Figure 4, d is the approximate distance between the adjacent CPPSs, $\overline{n}$ is the normal vector of CPPS on average.

This is to say, with geometric information of all the CPPSs, the best scanline of any ground point imaged is available by some computation based upon the space analytic geometry, which is fundamentally exempt from the computations of colinearity equations. Besides, the performance of the new method actually will not be affected by the terrain relief, as the classical colinearity constraints of the ground point, exposure station, and the corresponding image point are rigorously satisfied within the CPPS, no matter what the terrain conditions, judged from Figure 3 and Figure 4.

Representation of CPPS

Judging from the basic idea of the proposed method, it is a prerequisite step to collect the geometrical parameters of all CPPSs before the object-space BSS process is carried out. Nevertheless, the line sensor should not be directly processed as a straight line in practical utilizations (Tianen *et al.*, 2003; Zhang, 2005), and the definition of CPPS given above only exists in an ideal situation when hypothesizing the focal plane coordinates of all the CCD detectors of a line sensor could align with rigorous colinearity. However, this is hardly the case due to the several reasons, such as (a) the lens-distortion effect of the camera, (b) the unavoidable mounting error of CCD detectors on focal plane, and (c) the high-resolution airborne linear

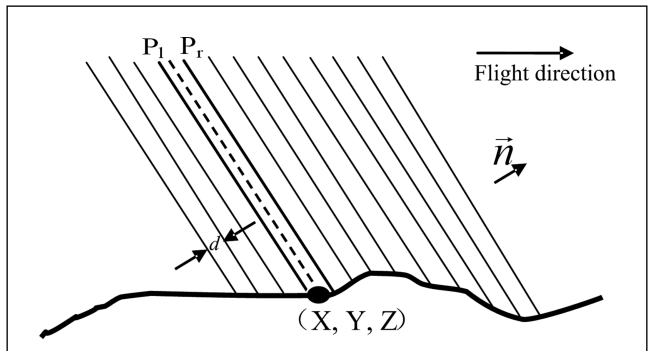

Figure 4. Principles of the best scanline search method based on CPPS Constraints of object space.

pushbroom cameras such as the ADS40 and STARIMAGER are all calibrated with focal plane coordinates of each CCD detector respectively provided. Therefore, the CPPS definition actually does not exist under this condition, or by definition, the CPPS is not ideally "plane" but irregular "surface" instead, which in fact results in rather complicated work for the rigorous parametric presentation of CPPS.

To make an objective analysis to the CCD deviation characteristics of the line sensor, the perpendicular distances from all CCD detectors to the base line which approximately represents the entire line sensor are computed to evaluate the sensor straightness. Here, let the base line be a straight line connecting detectors at both ends of the line sensor, and then computations are made on calibration data of each line sensor. Table 1 lists the maximum CCD deviation value of each line sensor of ADS40 camera tested.

It has been that found that the nadir sensors of ADS40 camera such as GRNN00A, BLUN00A, and REDN00A have relatively high straightness with a maximum CCD deviation around one detector size (0.0065mm), while the straightness of other sensors with slant viewing-angles is comparably lower, with the maximum CCD deviation reaching nearly 80 detector sizes (e.g., NIRF18A). Besides, although the maximum deviation degree varies with different sensor lines, the integral deviation trend of each sensor is smooth with almost one mild mode at the center section. All the above results demonstrate that the provided camera calibration data have considered the many inherent factors such as the lens-distortion, the CCD mounting error, etc. As illustrated in Figure 5, the curve shows the global deviation tendency of all CCD detectors' focal plane coordinates, where the back-viewing panchromatic-channel sensor named as PANB14A is taken as a case study.

To represent the geometric information of each CPPS, the geometric feature of the line senor should be determined or extracted in advance. The simplest way is using the straight line connecting detectors at both ends of the sensor to abstractly represent the total number of discrete CCD detectors. And then, based on such hypothesis, the geometric parameters of all the CPPSs are computed in collaboration with the sensor orientation information. Unfortunately, however, the simplest preprocess will not achieve the best search efficiency. Referring to the principles of the CPPS-based object-space BSS, it is evident that the correctness of the final results from object-space search process has a close linkage with the approaching degree of the hypothetical CPPSs with the real ones. For the line sensor that cannot be regarded directly as an ideally straight line, scanline compensation aiming at the CPPSs-based object-space search result is required to achieve the high search accuracy. The computation amount of compensation rigorously based on the colinearity equations is in proportion with the deviation degree of imaging detector from the ideally straight sensor line; the larger the deviation value, the more computation amount is required.

TABLE 1. THE CCD DEVIATION PARAMETERS (CAMERA NAME: ADS40_30027)

Sensor	Angle of view (deg.)	Maximum CCD Deviation (mm)
PANB14A	BACKWARD 14	0.541549
PANF28A	FORWARD 28	0.186345
NIRF18A	FORWARD 18	0.619620
GRNF16A	FORWARD 16	0.572124
GRNN00A	NADIR	0.007917
BLUN00A	NADIR	0.007685
REDN00A	NADIR	0.007607

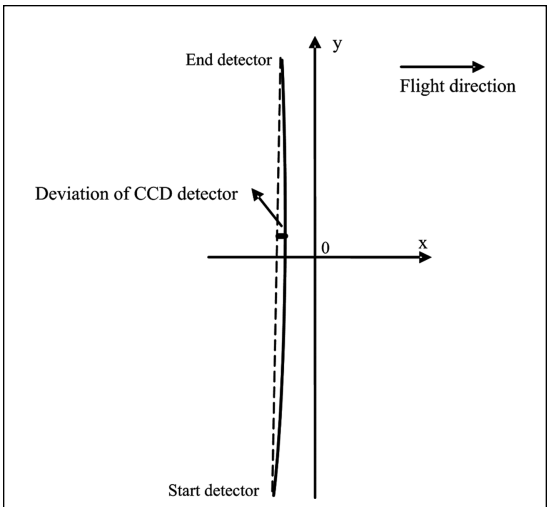

Figure 5. CCD coordinate deviation trend of the sensor line (PANB14A).

Nevertheless, just taking the characteristics of ADS40 camera into account (see Table 1 and Figure 5), it is impossible to restrict deviations of all detectors to only a few (less than one or two) detectors' size by fitting just one straight line to approximately represent al of the whole 12,000 detectors belonging to each sensor. Therefore, we attempt to use a more effective solution, where the whole CCD linear array is divided into several segments and with a straight line approximately presenting each of them. In this way, CPPSs are computed for each CCD line segment, based on which the BSS shall be carried out. The sensor segmentation strategy can considerably restrict deviation degree of CCD detectors, thus minimizing the compensation cost to the most degree.

As illustrated in Figure 6, take the straight line *AB* connecting the both ends of the original sensor as base line

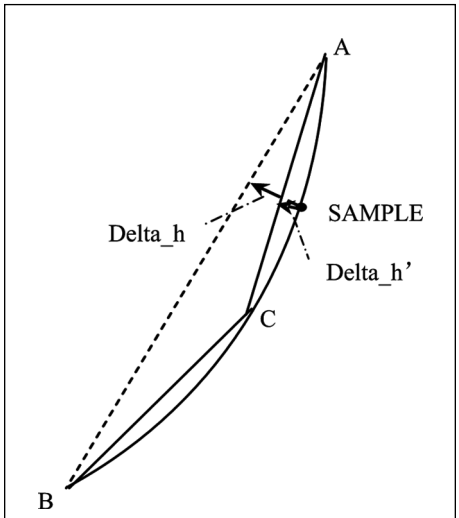

Figure 6. Sensor segmentation (Delta_h and Delta_h' respectively indicate the deviation value of detector SAMPLE respectively before and after segmentation).

and hypothesize that the CCD deviation reaches the peak value at detector *C*, at which the entire sensor will be divided into two segments. If the straight line connecting the both ends is regarded as the simplified presentation of each segment, accordingly there are two groups of CPPSs separately with a straight line *AC* and a straight line *CB*. As for detector indexed with *SAMPLE*, straight line *AC* instead of *AB* is adopted as base line for evaluating the CCD deviation value after sensor segmentation. Obviously, the computed deviation value is much smaller than that before segmentation. Further segmentation can continuously executed on each segment currently obtained until deviations of all detector are less than the demanded threshold (commonly one detector size). Thus, the computation cost for scanline compensation could be minimized.

Our BSS Strategy

Derived from the above analysis, the realization of the BSS method based on the CPPSs constraints mainly follows three stages: (a) computing parameters of CPPSs, (b) searching the best scanline based on CPPSs, and (c) compensating computation for the accurate value of best scanline.

Computing Parameters of CPPSs

This is a preprocess stage. To calculate parameters of CPPSs within one scene of image, the following three computation steps will be carried out only once, and then the obtained CPPSs parameters are directly used by each best scanline search:

Step 1
Segment the corresponding imaging line sensor. Based on the calibrated focal plane coordinates of each CCD detector, the famous Douglas-Peuker algorithm (Douglas and Peuker, 1973) is adopted to segment the original line sensor into *N* line segments. Use the straight line connecting detectors at both ends of each segment to approximately present each linear array. Therefore, there are *N* CPPSs for each scanline.

Step 2
Let $A \times X + B \times Y + C \times Z + M = 0$ be the plane equation of the CPPS, and the coefficients of the equation are computed by:

$$\begin{aligned} (A, B, C) &= \overline{n} \\ M &= -A \times Xs - B \times Ys - C \times Zs \end{aligned} \tag{2}$$

where, *A*, *B*, *C*, *M* are the coefficients of the CPPS equation, $\overline{n}$ is the normal vector of the CPPS, and *Xs*, *Ys*, *Zs* are the coordinates of the corresponding projection center.

Step 3
Calculate an estimated value for distance between the neighboring CPPSs. As symbol *d* shown in Figure 4, this parameter plays an important role in the object-space search process which accelerates the convergence speed of iterations. Although the aircraft speed can hardly be kept absolutely constant due to influences such as low-level airflow, it is still feasible to objectively measure such a variable on average, referred from the rules kept by flying platform. As for one scene of linear pushbroom image, parameter *d* can be computed with any of the following equations:

$$d = \frac{D_{se}}{N-1} \tag{3}$$

$$d = g \tag{4}$$

$$d = g \times \cos\alpha \tag{5}$$

where D_{se} is the distance from the exposure station of the last scanline to CPPS of the first scanline, *N* is the total number of scanlines contained in an image, *g* represents the Ground Sampling Distance (GSD), α is the viewing-angle of the corresponding line sensor, and *d* is the estimated distance of the neighboring CPPSs on average.

Searching the Best Scanline Based on CPPSs

This stage is essential to our method. The following steps are carried out to search for the best imaging scanline of a given ground point based on geometric information of CPPSs:

Step 1
Decide the imaging sensor segment of the ground point. Estimate the pixel coordinates of the ground point by two-dimensional object-to-image affine transformation, and the six global transformation parameters can be easily obtained while computing the parameters of CPPSs. Based on the estimated pixel coordinates (*l*, *s*), the sensor segment to which the imaging detector indexed with *s* belongs can be determined, and only CPPSs of this segment will be chosen for the object space BSS process.

Step 2
Hypothesize that the ground point is located between two adjacent CPPSs separately symbolized with P_l and P_r (see Figure 4). Search P_l and P_r which have the indexes *i* and $i+1$.

1. Compute the initial value of *i*, which is equivalent with *n* computed by:

$$n = (\text{int})\frac{D}{d} \tag{6}$$

   In this equation, *n* is the estimated count of scanlines between the ground point and the first CPPS of the image, initially *D* is the distance from the ground point to the first CPPS of the image, and *d* is the approximate distance between the neighboring CPPSs.
2. Iteratively verify the spatial relationship between the ground point and CPPSs indexed with *i* and $i+1$. That is, suppose $V_l = A_l \times X + B_l \times Y + C_l \times Z + M_l$, $V_r = A_r \times X + B_r \times Y + C_r \times Z + M_r$, where *X*, *Y*, *Z* are coordinates of the ground point, A_l, B_l, C_l, M_l are the equation coefficients of CPPS indexed with *i*, A_r, B_r, C_r, M_r are the equation coefficients of CPPS indexed with $i+1$. If $V_l \times V_r > 0$, self-increase or self-decrease the value of *i* according to the following rules:

$$\begin{aligned} V_l < 0 &\Rightarrow i = i - n \\ V_l > 0 &\Rightarrow i = i + n \end{aligned} \tag{7}$$

   where, *n* is the estimated count of scanlines between the ground point and CPPS indexed with *i*, which is also computed by Equation 6 in which *D* is the distance from the ground point to CPPS indexed with *i*.

   When $V_l \times V_r < 0$, it is demonstrated that the ground point is located between CPPSs indexed with *i* and $i+1$, i.e., P_l and P_r are determined, then the iteration is stopped.

Step 3
Interpolate the best scanline of the ground point, according to:

$$line = i + \frac{D_l}{D_l + D_r} \tag{8}$$

whereD_l is the distance from ground point to P_l, D_r is the distance from ground point to P_r, *i* is the index of P_l, and *line* is the object-space BSS result of the ground point.

Under the circumstance when the original line sensor itself can be directly processed as an ideally straight line,

the acquired value of *line* here is just the accurate value of best scanline.

Scanline Compensation

In most situations, the deviation of the CCD detectors should not be ignored for airborne linear pushbroom cameras, and the object space BSS result cannot achieve the desirable accuracy, due to the errors incurred from two aspects: the geometric inconsistency between the real irregular line sensor and the simplified one, and the underlying uncertainty in deciding the imaging sensor segment. Therefore, the value of *line* must be further compensated by rigorous *n*, so as to reach the required accuracy. The process of the colinearity equations-based compensation is the same as the traditional image space BSS process.

1. Based on the six orientation parameters of scanline *line*, calculate the image point coordinates (x, y) of the ground point with colinearity Equation 1; here y is the coordinate component in the direction of line sensor.
2. Calculate the detector index of (x, y), according to:

$$p = p_0 + (p_n - p_0)\frac{y - y_{p_0}}{y_{p_n} - y_{p_0}} \tag{9}$$

where p is the detector index, p_0,p_n are the detector indexes at both ends of the line sensor, and y_{p_0}, y_{p_n} are the focal plane coordinates of the detectors p_0,p_n in the direction of line sensor.

3. Suppose (x_s,y_s) are focal plane coordinates of detector p, the compensation value o is estimated as follows:

$$o = \frac{x - x_s}{c} \tag{10}$$

where c is the size of sensor detector.

Sensor segmentation is able to restrict the CCD deviation to the considerable degree (less than one sensor element size), thus, in most cases is able to ensure the sub-pixel accuracy of the object-space search result. Accordingly, it is demonstrated in practice that only one or at most two times of colinearity equation compensation is needed. Finally, to reach the even higher level search accuracy, the image-space scanline interpolation (Liu and Wang, 2007) is recommended.

Experimental Results

Test Datasets

In order to evaluate the performance of the developed technique, the proposed method has been applied to two types of linear pushbroom images captured by airborne ADS40 and STARIMAGER, respectively. The three scenes of L-0 level images with forward, nadir, and backward angle of view simultaneously captured in a flight strip have been used in the experiment. The image parameters are listed in Tables 2 and 3. The terrain type of ADS40 image data used here are mainly suburban mountainous area with a little terrain undulation, where the elevation difference between the minimum and the maximum is nearly 200 meters. As for image data of STARIMAGER, the terrain type is dominated with plain and farmland, with a subtle topographic relief of less than 40 meters.

TABLE 2. PARAMETERS OF ADS40 IMAGE DATA

Image	Angle of View (deg.)	Spectral Channel	Image Size
Forward	28	Panchromatic	40240 × 12000
Nadir	0	Green	40216 × 12000
Backward	14	Panchromatic	40232 × 12000

TABLE 3. PARAMETERS OF STARIMAGER IMAGE DATA

Image	Angle of View (deg.)	Spectral Channel	Image Size
Forward	14	Blue	49199 × 14404
Nadir	0	Blue	49199 × 14404
Backward	23	Blue	49199 × 14404

The experiment is carried out on each scene of image as follows. First, 1,000 columns × 10,000 rows with image coordinates (*Si*, *Li*) from each image are selected and projected onto the object-space horizontal planes with elevations randomly chosen from a specific elevation interval, hence simulating 10,000,000 number of corresponding ground points (*Xi*, *Yi*, *Zi*) (i = 1,2,3 . . . 10,000,000). Here, the range of the elevation interval is set between the minimum and maximum elevations of the image ground coverage.

Second, the CPPS Constraints based search, the bisecting window search, and the affine transformation based window search are respectively tested for object-to-image coordinate computation of the above simulated ground points. Their image coordinates (Si', Li') (i = 1,2,3 . . . 10,000,000) are calculated.

Finally, the value of each Li' with its theoretical value *Li* is compared to evaluate the correctness and accuracy of each search method. Besides, the total computation time with each search method is recorded, which serves as a reliable evaluation index of the search efficiency. The experimental results are listed in Tables 4 and 5.

In our experiment, all the developed programs are implemented in the Microsoft™ Visual C++ Integrated Development Environment on a desktop computer configured with the Microsoft™ XP Pro operating system, the Intel (R) Celeron(R) 2.80 GHZ CPU, and 2.79 GHZ, 512 MB volume of memory.

Results and Analysis

As shown in Tables 4 and 5, all the three search methods have achieved the desirable accuracy up to 0.01 pixel. A comprehensive analysis in both efficiency and robustness aspects is given as below, from which the superiority of the proposed method is demonstrated.

As mentioned in the previous sections of this paper, affine transformation based window search and bisecting window search are two typical optimized methods on the basis of the classical image-space solution strategy. Of these two methods, the bisecting window search is obviously more superior in the time-saving aspect, inferred from results illustrated in Table 3. By analysis, the time cost for each method is to a certain extent in direct proportion to the amount of colinearity equations-based computations. For each best scanline search, it needs about 25 times of colinearity equation-based computations on average with affine transformation based window search whereas 15 times with bisecting window search. Accordingly, the total time expenditure of affine transformation-based window search is nearly two times of that of bisecting window search, as shown in the table.

Compared with the bisecting window search, the proposed CPPS constraints based search method achieves not only the same accuracy level but also a much more desirable search speed, with time cost reduced by nearly

TABLE 4. EXPERIMENTAL RESULTS OF ADS40 IMAGES (10,000,000 POINTS)

Method	The proposed CPPS Constraints-based search		
Sensor	PANB14A	GRNN00A	PANF28A
Time(ms)	232,672	209,993	243,086
Times of colinearity equations computation for each search	1∼2	1∼2	1∼2
Count of sensor segments	16	2	23
The maximum error of scanline search	0.000527	0.000533	0.000856
Method	Affine transformation-based window search		
Sensor	PANB14A	GRNN00A	PANF28A
Time(ms)	2,405,672	2,392,351	2,442,155
Times of colinearity equations computation for each search	24∼26	24∼26	24∼26
The maximum error of scanline search	0.001212	0.000548	0.000648
Method	Bisecting window search		
Sensor	PANB14A	GRNN00A	PANF28A
Time(ms)	1,327,665	1,315,312	1,326,326
Times of colinearity equations computation for each search	14∼18	12∼17	14∼18
The maximum error of scanline search	0.000821	0.000648	0.001176

TABLE 5. EXPERIMENTAL RESULTS OF STARIMAGER IMAGES (10,000,000 POINTS)

Method	The proposed CPPS Constraints-based search		
Sensor	CCD_FB	CCD_NB	CCD_BB
Time(ms)	194,765	188,847	191,094
Times of colinearity equations computation for each search	1∼2	1∼2	1∼2
Count of sensor segments	2	1	2
The maximum error of scanline search	0.000454	0.000812	0.000543
Method	Affine transformation-based window search		
Sensor	CCD_FB	CCD_NB	CCD_BB
Time(ms)	2,314,794	2.495,426	2,503,523
Times of colinearity equations computation for each search	24∼26	24∼26	24∼26
The maximum error of scanline search	0.000915	0.000531	0.000549
Method	Bisecting window search		
Sensor	CCD_FB	CCD_NB	CCD_BB
Time(ms)	1,306,875	1,299,811	1,311,013
Times of colinearity equations computation for each search	13∼18	12∼17	14∼18
The maximum error of scanline search	0.000804	0.000612	0.000429

85 percent of the former. This is mainly due to that both sensor segmentation and the computation of CPPSs parameters are conducted only once in advance in the proposed method. That is, for each ground point, the CPPS-based search process simply involves small amount of calculations based on analytic geometry, and for further scanline compensation only one to two times of colinearity equation-based computations are most often needed.

According to the results, it can be concluded that the geometric straightness of STARIMAGER line sensor is prevailingly higher than that of ADS40 line sensor. In the experiments, with all of the detector deviations restricting within 0.004 mm (about two thirds of the ADS40 detector size and four fifths of the STARIMAGER detector size), the back, nadir, and forward sensors of ADS40 camera are respectively segmented into 16, 2 and 23 parts, whereas those of STARTIMAGER camera are segmented into only 2, 1, and 2 parts.

Derived from the experimental results, the number of the sensor segments does have some impact on the efficiency of CPPS constraints-based search process, and most often the larger the number, the more search time will be needed, as shown in Table 4 and Table 5. That is because theoretically if the original sensor is over-segmented, the segment interval will be correspondingly small, thus incurring relatively larger uncertainty for the correct choice of imaging segment. Fortunately, the post scanline compensation is able to deal with the error caused by incorrect segment selection; and it is the compensation efficiency, but not the accuracy, which is finally affected. Furthermore, experiments demonstrate that such effect is subtle. The experimental results of ADS40 images and STARIMAGER images also demonstrate that different terrain conditions will not affect the efficiency of the proposed search method.

Conclusions

This paper proposes a fast and efficient method for best scanline search issue of airborne linear pushbroom images on the basis of geometric constraints of object space. Based on the novel CPPSs constraints, the computation of parameters is finished during stage of preprocessing, which will be done only once. Additionally, the object-space best scanline search only needs some simple calculations on the basis of space analytic geometry, thus greatly improving the efficiency of best scanline search. The feasibility, robustness, and accuracy of the method are proved through experiments tested on datasets from the ADS40 and the STARIMAGER. Compared with the traditional methods, the search efficiency has been improved prominently, with time cost decreased by nearly 85 percent. Moreover, the higher the straightness degree of the sensor, the more perfect efficiency will be achieved. The proposed method has been successfully applied in the processing module of airborne linear pushbroom images developed by the State Key Laboratory of Information Engineering in Surveying, Mapping and Remote Sensing (LIESMARS), Wuhan University. It is manifested that the efficiency and robustness are all well guaranteed by adopting this new method in the object-to-image coordinate computation process.

Acknowledgments

The research described in this paper was funded by National Key Basic Research and Development Program of China (No. 2006CB701300) and National Key Technology R & D Program (2009AA12Z120).

References

Chen, T., R. Shibasaki, and Z. Lin, 2007. A rigorous laboratory calibration method for interior orientation of an airborne linear push-broom camera, *Photogrammetric Engineering & Remote Sensing*, 73(4):369–374.

Cramera, M, 2006. The ADS40 Vaihingen/Enz geometric performance test, *ISPRS Journal of Photogrammetry and Remote Sensing*, 60(6):363–374.

Douglas, D.H., and T.K. Peuker, 1973. Algorithm for the reduction of the number or points required to represent a digitized line or its caricature, *The Canadian Cartographer*, (10):47–55.

Fricker, P., 2001. ADS40 - Progress in digital aerial data collection, *Proceedings of Photogrammetric Week 2001* (D. Fritsch and R. Spiller, editors), Wichmann Verlag, Heidelberg, pp. 105–116.

Gruen, A., and L. Zhang, 2001. TLS data processing modules, *Proceedings of the 3rd International Seminar on New Developments in Digital Photogrammetry*, Gifu, Japan, pp. 69–70.

Gruen, A., and L. Zhang, 2002. Automatic DTM generation from three-line-scanner (TLS) images, *Proceedings of theGIT Kartdagar Symposium*, 17–19 April, Stockholm, Sweden, unpaginated CD-ROM.

Gruen, A., and L. Zhang, 2003. Sensor modeling for aerial triangulation with three-line-scanner (TLS) imagery, *Journal of Photogrammetrie, Fernerkundung, Geoinformation*, (2):85–98.

Haala, N., D. Fritsch, D. Stallmann, and M. Cramer, 2000. On the performance of digital airborne pushbroom cameras for photogrammetric data processing - A case study, *International Archives of Photogrammetry and Remote Sensing*, 33(B4/1):324–331.

Heier, H., M. Kiefner, and W. Zeitler, 2002. Calibration of the digital modular camera DMC, *Proceedings of the 22nd FIG International Congress*, 19–26 April, Washington, D.C., unpaginated CD-ROM.

Hinz, A., C. Dörstel, and H. Heier, 2000. Digital Modular Camera: System concept and data processing workflow, *International Archives of Photogrammetry and Remote Sensing*, 13–16 July, Amsterdam, 33(B2):164–171.

Koichi, T., A. Gruen., L. Zhang, M. Shunji, and S. Ryosuke, 2004. STARIMAGER - A new airborne three-line scanner for large-scale applications, *International Archives of Photogrammetry, Remote Sensing and Spatial Information Sciences*, 35(1):226–231.

Leberl, F., M. Gruber, and M. Ponticelli, 2003. Flying the new large format digital aerial camera UltraCam, *Proceedings of the Photogrammetric Week 2003*, Stuttgart, Germany, p. 67–76.

Leberl, F., R. Perko, M. Gruber, and M. Ponticelli, 2002. Novel concepts for aerial digital cameras., *International Archives of Photogrammetry, Remote Sensing and Spatial Information Sciences*, 34(1):10–15.

Liu, J., and D.H. Wang, 2007. Efficient orthoimage generation from ADS40 level0 products, *Journal of Remote Sensing*, 11(2):21–26.

Morgan, M., K. Kim, S. Jeong, and A. Habib, 2004. Epipolar geometry of linear array scanners moving with constant velocity and constant attitude, *International Archives of Photogrammetry, Remote Sensing and Spatial Information Sciences*, Istanbul, Turkey, 35(B2):418–423.

Murai, S., and Y. Matsumoto, 2000. The development of airborne three line scanner with high accuracy INS and GPS for analysing car velocity distribution, *International Archives of Photogrammetry and Remote Sensing*, Amsterdam, Vol. 33, Part B2, pp. 416–421.

Poli, D., 2005. *Modelling of Spaceborne Linear Array Sensors*, Ph.D. Dissertation, Institute of Geodesy and Photogrammetry, ETH Zurich, IGP Mitteilungen Nr. 85, 217 p.

Reulke, R., K.-H. Franke, P. Fricker, T. Pomierski, R. Sandau, M. Schoenermark, C. Tornow, and L. Wiest, 2000. Target related multispectral and true color optimization of the color channels of the LH systems ADS40, *International Archives of Photogrammetry and Remote Sensing*, Amsterdam, Vol. 33, Part B1, pp. 244–250.

Reulke, R., S. Becker, N. Haala, and U. Tempelmann, 2006. Determination and improvement of spatial resolution of the

CCD-line-scanner system ADS40, *ISPRS Journal of Photogrammetry and Remote Sensing*, (60):81–90.

Sandau, R., B. Braunecker, H. Driescher, A. Eckardt, S. Hilbert, J. Hutton, W. Kirchhofer, E. Lithopoulos, R. Reulke, and S. Wicki, 2000. Design principles of the LH systems ADS40 airborne digital sensor, *International Archives of Photogrammetry and Remote Sensing*, 33(B2):258–265.

Tianen, C., S. Ryosuke, and S. Murai, 2003. Development and calibration of the airborne scanner (TLS) imaging system, *Photogrammetric Engineering & Remote Sensing*, 69(1):71–78.

Wolf, P.R., and B.A. Dewitt, 2000. *Elements of Photogrammetry with Applications in GIS*, Third edition, McGraw-Hill, Toronto, 608 p.

Zhang, L., 2005. Automatic *Digital Surface Model (DSM) Generation from Linear Array Images*, Ph.D. Dissertation, Institute of Geodesy and Photogrammetry, ETH Zurich, Switzerland, IGP Nr. 16078, 199 p.

Zhao, S. M., and D.R. Li, 2006. Geometric pre-process of ADS40, *Geomatics and Information Science of Wuhan University*, 31(4):308–311.